

# A Modified Metal-Oxide Memristor Model for Reconfigurable Filters

Ivan D. Zaykov

**Abstract** — Memristor elements are innovative and nano-dimension electronic nonlinear two-terminal components with memory effect, and have potential application in various electronic circuits, like memory devices, neural nets, digital and analog reconfigurable schemes, which engineering involves accurate and simplified models. In this work, a modified and better-quality model for metal oxide-based memristor elements is presented, to be applied for primary design of memristor-based analog filters. The presented memristor model has a high correctness, simple mathematical equations and sensitivity thresholds. Its LTSPICE library model is created and used for investigations of low-pass and high-pass analog filters. The offered memristor model suitably represents the nonlinear dopant motion. The corresponding voltage-current and state-flux relations are analyzed for both hard-switching and soft-switching regimes. The conducted analyses and computer simulations approve its proper operation in electronic devices, expressing the basic and important fingerprints of memristor components.

**Index Terms** — metal oxide-based memristors, nonlinear dopant drift, sensitivity thresholds, LTSPICE model, filters

## I. INTRODUCTION

In the last several years, the resistance switching in some oxide thin films, based on transition metals has been intensively analyzed [1,2]. The switching effects are accompanying to the change of the oxide conductance with the applied voltage signal and the stored electric charges [3]. Such chemical mixtures can hold their resistance for a long-time interval after the energy sources are switched off [4]. The collected charges are proportional to the time integral of the electric current [5]. Due to this very useful property, the oxides founded on transition metals as  $\text{HfO}_2$ ,  $\text{TiO}_2$ ,  $\text{NbO}$ ,  $\text{Ta}_2\text{O}_5$ , and many others might be used as storing cells in memory circuits [6, 7, 8]. The presence of the fourth basic one-port passive and nonlinear electronic element – the *memristor*, together with the capacitor, inductor and resistor, is projected by Chua in 1971, rendering to symmetry considerations [9]. The first physical memristor is fabricated by titanium dioxide in Hewlett-Packard investigation labs controlled by Williams in 2008 [10]. Several scientific teams attempted to fabricate memristive components, based on various materials and techniques [11, 12]. Several various categories of memristor elements, made of polymeric mixtures, spintronic and magnetic materials [13], amorphous  $\text{SiO}_2$  [14] and others are designated in the research

works [15]. The fundamental and valued properties of memristors are their non-volatile memory effect, low energy usage, nano-sizes, higher switching speed, and a sound compatibility to Complementary Metal Oxide Semiconductor (CMOS) integrated circuits [15, 16]. These memristor features are in agreement with their potential applications in neural nets, memory circuits [16, 17], analog and digital electronic devices, and other electronic schemes [15, 18]. The construction of electronic circuits requires their previous analysis by simulations [19, 20, 21]. Compared to the other SPICE products, LTSPICE is a preferable one for researches due to its simple design, user-friendly interface, and free license [20]. Several precise models of  $\text{Ta}_2\text{O}_5$ ,  $\text{TiO}_2$ ,  $\text{HfO}_2$ , and other memristors are available in the literature [22, 23, 24]. These elements are comparatively different, according to some construction's specifics, functional operation and efficiency in electric field [24, 25]. But, in many occasions general memristive models might be used for a broad class of transition metal oxide-based memory elements. The specialized and high-precision models of metal oxide memristors are at times very complex for SPICE inclusion [26, 27, 28, 29]. The main aim of this work is to suggest a simple, high-accuracy, fast-operating and universal LTSPICE memristor model, appropriate for analysis and simulation of a broad class metal-oxide memristors. The offered simple and enhanced model, denoted as  $B_{15}$  is mainly based on Lehtonen-Laiho model [23] and the simplified structure of tantalum oxide memristors [7,8]. It has simple mathematical equations, respectable accuracy and fast functioning in SPICE simulation software, which are its basic advantages, with respect to various existing models [6, 14]. Another pro of the offered model is the use of activation (sensitivity) threshold, which ensures its applicability in neural nets and memory devices [11]. The proposed model is applied and analyzed in simple analog filters [30, 31]. Comparing to experimental current-voltage relations [6, 7] and to those obtained by some frequently applied memristor models [14], it could be concluded that the proposed model has a good precision. For control the state variable and illustration the boundary condition effects at hard-switching operation, a modified Bielek window [14] is used. For avoidance of convergence issues in SPICE, a flat and differentiable sigmoidal function is applied.

Section 2 represents a short clarification of the fundamental metal oxide-based memristors and the respective modeling. The offered general memristive model is explained in Section 3. The related LTSPICE library model is expressed and commented in Section 4. Its incorporation in simple analog filters is presented in Section 5. Section 6 represents the conclusion.

The paper is resubmitted after review on 11.04.2022.

I. D. Zaykov is with the Department Fundamentals of Electrical Engineering, Technical University of Sofia, 1000 Sofia, Bulgaria (e-mail: ivanzaykov@tu-sofia.bg).

## II. A BRIEF OVERVIEW OF METAL OXIDE-BASED MEMRISTORS AND THEIR MODELING

For good understanding of memristor's modeling and functioning, a description of the metal-oxide memristors is firstly presented. The state variable for HfO<sub>2</sub> and TiO<sub>2</sub>-based memristors is a ratio between the sizes of the doped layer and those of the memristor [7, 10]. A simplified structure of metal oxide memristor is shown in Fig. 1 a). It contains two terminals - top electrode, (*anode*) and bottom electrode (the *cathode*). The central region is doped by oxygen vacancies and has a high conductance, while the peripheral part is with a lower conductance. The applied voltage causes the change of the area of the conducting region [7]. For Ta<sub>2</sub>O<sub>5</sub> memristor components, the state variable is a ratio between the surfaces of the central part  $a_1$  and those of the whole intersection  $a_2$  [7].

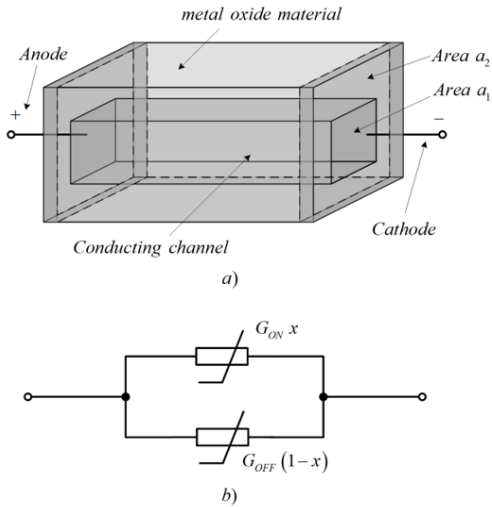


Fig. 1. A simplified physical structure of metal oxide memristor

The state variable of the memristor  $x$  then might be expressed by the following equation (1) [7]:

$$x = \frac{a_1}{a_2}, 0 \leq x \leq 1 \quad (1)$$

The state-dependent relation between the voltage  $v$  and the respective current  $i$ , according to the equivalent schematic presented in Fig. 1 b) is [7, 14]:

$$i = G(x)v = [G_{ON}x + G_{OFF}(1-x)]i \quad (2)$$

Here,  $G(x)$  is the conductance of the memristor element, also known as a *memductance* [10]. The math expressions that entirely describe a memristor element involve a *state differential equation*, which relates the time derivative of  $x$  and the voltage (current), and the current-voltage expression, dependent on memristor *state* [10]:

$$\begin{cases} x' = k f_B(x, i) i \\ i = G(x) i \end{cases} \quad (3)$$

where  $f(x, i)$  is a *window*, used for restriction of  $x$  in the range (0,1) and for representing of the border effects, and  $k$  is a coefficient, based on the properties of the memristor.

The oxygen vacancies *mobility* denoted by  $\mu$  is dependent on the applied voltage. When the *electric field intensity*

exceeds a given threshold, the ionic mobility increases exponentially [1, 14]. The processes combined with this effect are quite complex and might not be correctly presented, using a simplified memristive model.

The Lehtonen-Laiho model is applied for investigation of metal oxide-based memristors [23]. It is with a high precision and properly presents the nonlinear ionic dopant motion. This memristor model is expressed by the presented equations' set [23]:

$$\begin{cases} i = \chi [\exp(\gamma v) - 1] + x^n \cdot \beta \cdot \sinh(\alpha v) \\ \frac{dx}{dt} = a \cdot f_B(x, i) \cdot v^m \end{cases} \quad (4)$$

where  $\chi, \gamma, \beta, n, \alpha, a$  and  $m$  are parameters for fitting of the memristive model [23]. The first term in (4) shows the quick increase of the current with the applied voltage, while the next one describes its dependence on the memristor state [5, 23]. For simplifying of the offered memristor model, a rough representation of the nonlinear ionic drift [1] is shown in the following section.

## III. THE PROPOSED OXIDE-BASED MEMRISTOR MODEL

The suggested memristor model is fully presented by equation (5). The ON-state and OFF-state conductances are denoted by  $G_{ON}$  and  $G_{OFF}$ , respectively. The coefficients  $k_1$  and  $k_2$  are applied in the memristor model for its tuning.

$$\begin{cases} i = G(x)v = [G_{ON}x + G_{OFF}(1-x)]v \\ \frac{dx}{dt} = 0, \quad |v| < v_{thr} \\ \frac{dx}{dt} = k_1(k_2 v)^3 f_J(x), \quad |v| \geq v_{thr} \\ f_J(x) = 1 - (2x - 1)^{2p} \end{cases} \quad (5)$$

The first equation presents the relationship between the current  $i$  and the voltage  $v$ . The second relation contains the *sensitivity threshold*  $v_{thr}$ , and according to this expression, the state variable  $x$  has a constant value, when the voltage is lower than this level. The third expression in (5) relates the time derivative of  $x$  and the voltage. The expression  $k_2 \cdot v^3$  is included for approximate representation of the nonlinear dopant motion [1]. The included in (5) Joglekar window is limiting the *state variable* in the interval [0, 1] [14].

The proposed memristor model is investigated at sinusoidal voltage signals for both *hard-switching* and *soft-switching* functioning. The values of the model's parameters are derived by parameter estimation, based on simulation annealing and gradient descent of the root mean square error between the experimental and simulated memristor currents [6, 7]. The values of the coefficients are:  $k_1 = 715.3$ ,  $k_2 = 1.49$ ,  $m = 1.03 \cdot 10^{-7}$ ,  $x_0 = 0.43$ ,  $G_{ON} = 0.011$ ,  $G_{OFF} = 0.00013$ ,  $v_{thr} = 0.11$ ,  $p = 10$ . The voltage-current and state-flux relationships of the suggested model are presented in Fig. 2, together with these of Lehtonen-Laiho, Biolek and Joglekar models for comparison the results. In this case, the memristor models are operating in a soft-switching mode and the behavior of Joglekar and Biolek models is almost

identical. Owing to this, the respective graphics of the models almost match one to another.

The corresponding time diagrams of the voltage, current, and state variable are shown in Fig. 3. The time for simulation of the offered model is about 18.4 ms, for Lehtonen-Laiho model it is about 19.7 ms, for Joglekar model [32] – 16.1 ms and for Biolek model – 16.6 ms. The respective errors are: 2.74 % for the suggested model, 2.66 % for Lehtonen-Laiho model, 3.62 % for Joglekar model and 3.46 % for Biolek model. It could be stated that, rendering to the errors and simulation times, the presented memristive model has a sound accuracy, near to those of Lehtonen-Laiho model, and it is with a lower time for simulation. Based on the equations of the proposed model, the corresponding LTSPICE memristor library model is created and presented in the next section.

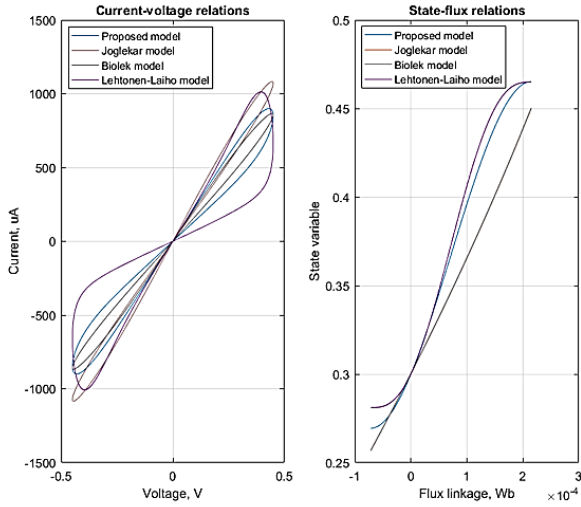


Fig. 2. Current-voltage and state-flux relations according to the suggested memristor model, Joglekar, Lehtonen-Laiho and Biolek memristor models

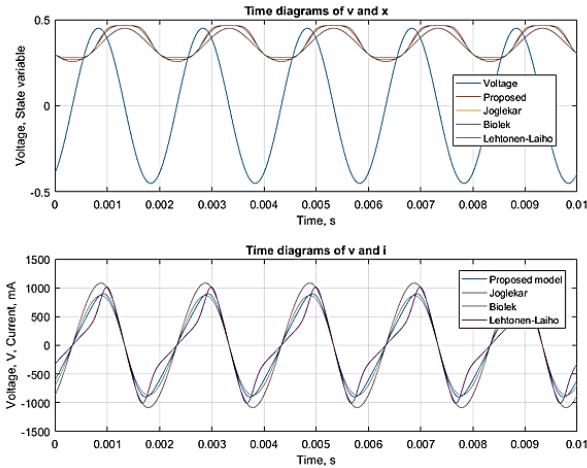


Fig. 3. Time diagrams of the memristor voltage and currents according to the proposed model, Joglekar, Lehtonen-Laiho and Biolek models

#### IV. THE LTSPICE LIBRARY MEMRISTOR MODEL

Based on the presented memristor model, expressed by (5), a corresponding LTSPICE [20] memristor model is created. The mainly used blocks in LTSPICE [20] are applied for expressing of the mathematical operations, correspondent to the considered memristor model.

The LTSPICE code of the described metal oxide memristive model is shown as follows:

```
.subckt B15 te be Y
.param k1=1500 k2=1.1 gon=0.01 goff=0.0001
.param m=1.2e-8 vthr=0.1 pp=10
Cint Y 0 1 IC=0.3
Rad Y 0 100G
Gy 0 Y value={k1*pow((k2*V(te,be)),3)*
(1-pow((2*V(Y)-1),(2*pp)))*
(stpp((abs(V(te,be))-vthr), m))}
G1 te be value={V(te,be)*(gon*V(Y)+goff*(1-V(Y)))}
.func stpp(x,p)={0.5*(1+(x/sqrt(pow(x,2)+p)))}
.ends B15
```

The state variable is proportional to the voltage  $V(Y)$  of the element  $C_1$  [5, 14]. The current through the capacitive element expresses the time derivative of  $x$ . The voltage-controlled source  $G_1$  presents the memristor current. The resistor  $R_1$ , coupled parallelly to  $C_1$  decreases the probability for occurrence of convergence problems [14]. The electrodes of the element are the *anode (top electrode, te)* and the *cathode (bottom electrode, be)*. The terminal  $Y$  is applied for detection of the state variable  $x$ .

The created LTSPICE model is tested under pulse regime and by sine voltages with different frequencies. The LTSPICE model is attached in a circuit for analysis of its behavior, given in Fig. 4 for presentation of its elements and contacts. The electrode  $Y$  is attached to a resistor with a high value  $R_1$ , which prevents the alteration of the memristor state variable. The source  $B_1$  creates a signal, proportional to the respective *flux linkage*.

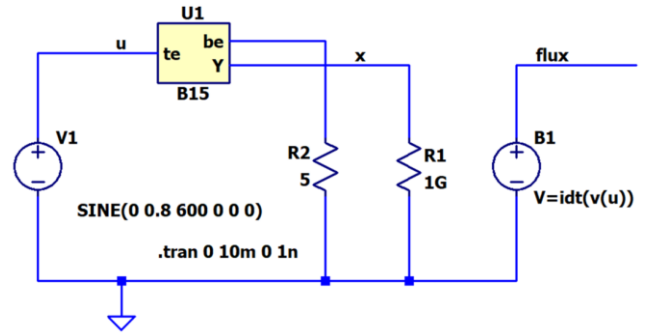


Fig. 4. A circuit for analysis of the offered model, containing a voltage source  $V_1$  and integrating element  $B_1$  for the flux linkage

The obtained  $i-v$  characteristics are given in Fig. 5 for approval of the model's proper operation. It is visible that, when the frequency of the voltage increases, then the area of the respective current-voltage hysteresis decreases. This is in agreement with the basic fingerprints of the memristors [14, 18]. The memristor model is also tested under *pulse mode*, presenting both hard-switching and soft-switching states. The simulation time of the proposed model is 17.4 ms. According to Lehtonen-Laiho memristor model [23], the offered here model is with a lesser simulation time, due to its simplified equations and reduced number of math operations. The precision of the suggested memristor model is very close to those of Lehtonen-Laiho memristive model, according to the RMS error.

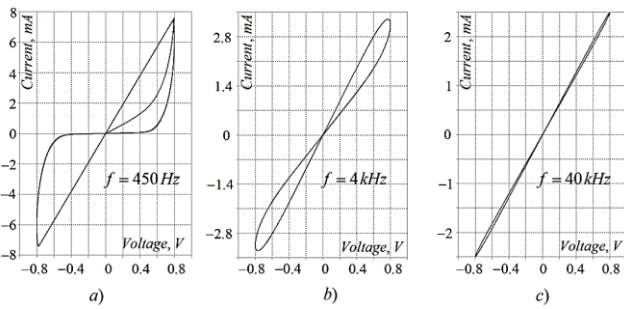


Fig. 5. Current-voltage characteristics, obtained by the offered memristor model at various frequencies a)  $f = 450$  Hz; b)  $f = 4$  kHz; c)  $f = 40$  kHz

## V. LOW-PASS AND HIGH-PASS ANALOGUE FILTERS BASED ON MEMRISTORS

The described in this section analog and passive low-pass and high-pass filters are based on resistor-capacitor series circuits, where the resistors are replaced by memristor elements. In the considered filtering circuits, the use of inductances is avoided [30, 31]. The filters are presented in Fig. 6 for additional description of their operation and main features. Fig. 6 a) represents a low-pass filter, where the output voltage is the voltage drop across the capacitor  $C_1$ .

The resistances of the memristors  $M_1$  and  $M_2$  are tuned by external voltage pulses. The load resistances are with a very high value and are not shown in the schematics. The respective high-pass filter is depicted in Fig. 6 b) and the output voltage in this case is the voltage drop across the memristive element  $M_2$ . The capacitors  $C_1$  and  $C_2$  have a capacity of 1 nF.

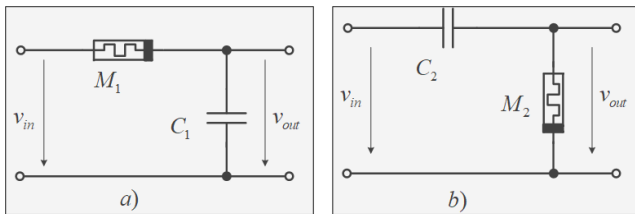


Fig. 6. a) A memristor-based low-pass filter; b) High-pass analog filter based on memristor and capacitor

The cut-off frequency of the memristor-based low pass filtering circuit is dependent on the resistance of the memristor  $M_1$  and the capacitance  $C_1$  [5, 31] and it is altered by the change of the memristance  $M_1$ , using external signals:

$$f_{cut-off\ low} = \frac{1}{2\pi M_1 C_1} \quad (7)$$

The cut-off frequency of the high-pass filtering group is presented below [30, 31]:

$$f_{cut-off\ high} = \frac{1}{2\pi M_2 C_2} \quad (8)$$

and it is adjusted by external voltage pulses, affecting the memristance  $M_2$ . The amplitude-frequency responses and the correspondent phase-frequency characteristics of the considered memristor-based analog filters are presented in Fig. 7 a) and Fig. 7 b) for expression of the respective characteristics and properties. The cut-off frequency is about 850 MHz and the correspondent value of the state variable is  $x = 0.32$ , the respective memristance is about 9.34 k $\Omega$ .

Based on the presented schematics of the considered filtering groups, different types of complex filtering circuits could be constructed, as band-pass and band-stop filters.

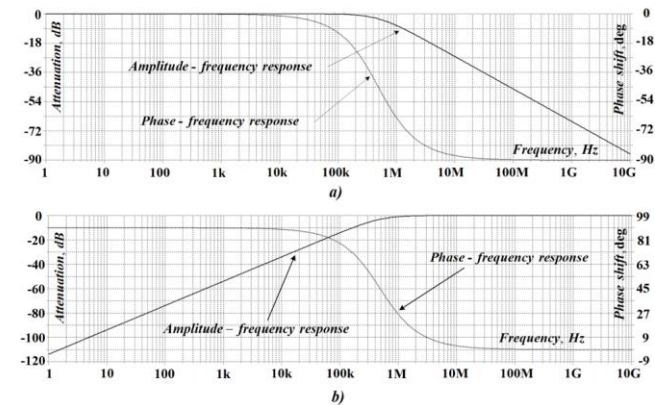


Fig. 7 a) Amplitude-frequency response and phase-frequency response of the low-pass memristor filter presented in Fig. 6 a); b) Amplitude-frequency and phase-frequency responses of the high-pass filter - Fig. 6 b)

## VI. CONCLUSION

The suggested modified and improved metal oxide-based memristor model is mainly founded on the standard Lehtonen-Laiho memristive model, including a simplified and highly nonlinear relationship between the time derivative of the state variable  $x$  and the applied voltage. It permits the memristor model to correctly operate at higher frequencies. Founded on the presented metal oxide memristor model, denoted by  $B_{15}$ , low-pass and high-pass filters are analyzed and their operation is presented, paying attention on their main pros, rendering to their classical capacitor-resistor analogues. The proper operation of the offered memristor model is established by a comparison to several classical memristor models, as these of Joglekar, Biolek and Lehtonen-Laiho.

Due to the usage of activation threshold, the considered modified memristor model is successfully included in programmable memristor-based analog filters. In the normal operating regime of these filtering groups, when the memristor voltage is lower than the activation threshold, then the memristance is a constant and the filters operate as simple and linear circuits. For adjustment of the cut-off frequencies and the respective bands of the circuits, external voltage pulses are used for changing the resistance of the memristor elements. Nevertheless, for high-frequency signals the Joglekar and Biolek memristor models are able to properly operate in the presented filtering circuits, the offered memristor model  $B_{15}$  has better representation, according to the linearity of the filtering devices, owing to the use of sensitivity thresholds.

## REFERENCES

- [1] Strukov, D.B., Williams, S., "Exponential ionic drift: Fast switching and low volatility of thin-film memristors," *Applied Physics A* 2009, pp. 515–519, <https://doi.org/10.1007/s00339-008-4975-3>
- [2] Chiu, F.C. „A Review on Conduction Mechanisms in Dielectric Films,“ In *Advanced Materials Science Engineering*; Hindawi Publishing Corporation: London, UK, 2014; Vol. 2014, pp. 1–18, <https://doi.org/10.1155/2014/578168>
- [3] Mohammad, B., Jaoude, M., Kumar, V., Al Homouz, D., Nahla, Heba Abu, Al-Qutayri, M., Christoforou, N., "State of the art of metal oxide memristor devices," *Nanotech. Rev.*, vol. 5, no. 3, 2016, pp. 311-329, <https://doi.org/10.1515/ntrev-2015-0029>

- [4] Wang, X., Chen, Y., Xi, H., Li, H., Dimitrov, D., "Spintronic Memristor Through Spin-Torque-Induced Magnetization Motion," *IEEE Electron Device Lett.* 2009, 30, pp. 294–297, <https://doi.org/10.1109/LED.2008.2012270>
- [5] Mladenov, V., "Advanced Memristor Modeling—Memristor Circuits and Networks," MDPI: Basel, Switzerland, 2019; p. 172. ISBN 978-3-03897-104-7 (Hbk).
- [6] Amer, S., Sayyaparaju, S., Rose, G., S. Beckmann, K., Cady, N.C., "A practical hafnium-oxide memristor model suitable for circuit design and simulation," In 2017 IEEE (ISCAS) 2017 May 28, pp. 1-4, DOI: 10.1109/TCT.1971.1083337.
- [7] Strachan, J., Torrezan, A., Miao, F., Pickett, M., Yang, J., Yi, W., Medeiros-Ribeiro, G., Williams, R.S., "State Dynamics and Modeling of Tantalum Oxide Memristors," *IEEE Transactions on Electron Devices*, 2013, pp. 2194–2202, <https://doi.org/10.1109/TED.2013.2264476>
- [8] Mladenov, V., Kirilov, S., "A Simplified Model of Tantalum Oxide Based Memristor and Application in Memory Crossbars," 2021 10th International Conference on Modern Circuits and Systems Technologies (MOCAS), 2021, pp. 1-4, doi: 10.1109/MOCAS52088.2021.9493384.
- [9] Chua, L. "Memristor - The missing circuit element," *IEEE Trans. Circuit Theory* 1971, 18, pp. 507–519, <https://doi.org/10.1109/TCT.1971.1083337>
- [10] Strukov, D. B., Snider, G. S., Stewart, D. R., Williams, S., "The missing memristor found," *Nature* 2008, 453, pp. 80–83, <https://doi.org/10.1038/nature06932>
- [11] Solovyeva, E. B., Azarov, V. A., "Comparative Analysis of Memristor Models with a Window Function Described in LTspice," 2021 IEEE Conference of Russian Young Researchers in Electrical and Electronic Engineering (EIConRus), 2021, pp. 1097-1101, doi: 10.1109/EIConRus51938.2021.9396217.
- [12] Chen, Y., Liu, G., Wang, C., Zhang, W., Li, R.-W., Wang, L., "Polymer memristor for information storage and neuromorphic applications," *Mater. Horizons* 2014, 1, pp. 489–506, <https://doi.org/10.1039/C4MH00067F>
- [13] Mladenov, V., Kirilov, S., "A Simplified Tantalum Oxide Memristor Model, Parameters Estimation and Application in Memory Crossbars," *MDPI Technologies* 2022; 10 (1), 6. <https://doi.org/10.3390/technologies10010006>.
- [14] Ascoli, A., Corinto, F., Senger, V., Tetzlaff, R., "Memristor Model Comparison," *IEEE Circuits Syst. Mag.* 2013, 13, pp. 89–105, <https://doi.org/10.1109/MCAS.2013.2256272>
- [15] Ascoli, A., Tetzlaff R., Corinto, F., Mirchev, M., Gilli, M., "Memristor-based filtering applications," 2013 14th Latin American Test Workshop - LATW, 2013, pp. 1-6, doi: 10.1109/LATW.2013.6562672.
- [16] Kirilov, S., Mladenov, V., "Integrator device with a memristor element," 2018 7th International Conference on Modern Circuits and Systems Technologies (MOCAS), 2018, pp. 1-4, doi: 10.1109/MOCAS.2018.8376656.
- [17] Mladenov, V., Kirilov, S., "Learning of an Artificial Neuron with Resistor-Memristor Synapses," *ANNA '18; Advances in Neural Networks and Applications*, 2018, pp. 1-5.
- [18] Linn, E., Siemon, A., Waser, R., Menzel, S., "Applicability of Well-Established Memristive Models for Simulations of Resistive Switching Devices," *IEEE Trans. Circuits Syst.* 2014, 61, pp. 2402–2410, <https://doi.org/10.1109/TCSI.2014.2332261>
- [19] Yang, W. Y., Cao, W., Chung, Tae-Sang, Morris, J., "Applied numerical methods using MATLAB," John Wiley & Sons, Inc., ISBN 0-471-69833-4, 2020, pp. 509.
- [20] May, C., "Passive Circuit Analysis with LTspice® - An Interactive Approach," Springer Nature Switzerland AG 2020, ISBN 978-3-030-38304-6, <https://doi.org/10.1007/978-3-030-38304-6>, pp. 763.
- [21] Mladenov, V., "A Unified and Open LTSPICE Memristor Model Library," *MDPI Electronics*, 2021, Vol. 10, no. 13: 1594. <https://doi.org/10.3390/electronics10131594>, pp. 1 – 27.
- [22] Biolek, Z., Biolek, D., Biolkova, V., "SPICE Model of Memristor with Nonlinear Dopant Drift," *Radioengineering* 2009, 18, pp. 210–214.
- [23] Lehtonen, E., Laiho, M., "CNN using memristors for neighborhood connections," In *Proceedings of the 2010 12th (CNNA 2010), Berkeley, CA, USA, 3–5 February 2010*, pp. 1–4, <https://doi.org/10.1109/CNNA.2010.5430304>
- [24] Mladenov, V., Kirilov, S., "A Nonlinear Memristor Model with Activation Thresholds and Variable Window Functions," *CNNA 2016; 15th International Workshop on Cellular Nanoscale Networks and their Applications*, 2016, pp. 1-2.
- [25] Ascoli, A., Tetzlaff, R., Biolek, Z., Kolka, Z., Biolkova, V., Biolek, D., "The Art of Finding Accurate Memristor Model Solutions," *IEEE J. Emerg. Sel. Top. Circuits Syst.* 2015, 5, pp. 133–142, <https://doi.org/10.1109/JETCAS.2015.2426493>
- [26] Kirilov, S., Todorova, V., Nakov, O., & Mladenov, V., (). "Application of a Memristive Neural Network for Classification of COVID-19 patients," *International Journal of Circuits, Systems and Signal Processing*, 2021, 15, pp. 1282-1291, <https://doi.org/10.46300/9106.2021.15.138>
- [27] Abdalla, H., and Pickett, M. D., "SPICE modeling of memristors," 2011 IEEE International Symposium of Circuits and Systems (ISCAS), 2011, pp. 1832-1835, doi: 10.1109/ISCAS.2011.5937942.
- [28] Yakopcic C., Taha T. M., Subramanyam G., Pino R. E., "Memristor SPICE Modeling," In: Kozma R., Pino R., Pазienza G. (eds) *Advances in Neuromorphic Memristor Science and Applications*. Springer Series in Cognitive and Neural Systems, 2012, vol 4. Springer, Dordrecht. [https://doi.org/10.1007/978-94-007-4491-2\\_12](https://doi.org/10.1007/978-94-007-4491-2_12).
- [29] Batas D., Fiedler, H., "A Memristor SPICE Implementation and a New Approach for Magnetic Flux-Controlled Memristor Modeling," in *IEEE Transactions on Nanotechnology*, vol. 10, no. 2, pp. 250-255, March 2011, doi: 10.1109/TNANO.2009.2038051.
- [30] Winder, S., "Analog and digital filter design," 2002, Elsevier Science, USA, ISBN 0-7506-7547-0.
- [31] Lautaro Fernandez-Canque, H., "Analog Electronics Applications – fundamentals of design and analysis," CRC Press Taylor & Francis Group, ISBN 978-1-4987-1495-2, 2017.
- [32] Joglekar, Y., Wolf, S.J. "The elusive memristor: Properties of basic electrical circuits," *Eur. J. Phys.* 2009, 30, pp. 661–675, <https://doi.org/10.1088/0143-0807/30/4/001>